

CHAPTER 6

Characterization of the Ni-Fe active site and of the Fe-S clusters of the membrane-bound hydrogenase from *Ralstonia eutropha* by X-ray absorption spectroscopy

Simone Löscher^a, Marcus Ludwig^b, Antonio De Lacey^c, Holger Dau^a,
Bärbel Friedrich^b, Michael Haumann^{a,*}

^aFreie Universität Berlin, Institut für Experimentalphysik, Arnimallee 14, D-14195 Berlin, Germany;

^bHumboldt-Universität zu Berlin, Institut für Mikrobiologie, Chausseestr. 117, D-10115 Berlin, Germany;

^cInstituto de Catálisis, C.S.I.C., C/ Marie Curie s-n, Campus Universidad Autónoma-Cantoblanco, Spain

Keywords:

Bioinorganic chemistry, *Ralstonia eutropha*, membrane-bound Ni-Fe hydrogenase, X-ray absorption spectroscopy.

Abbreviations: EPR, electron paramagnetic resonance spectroscopy; EXAFS, extended X-ray absorption fine structure; FTIR, Fourier-transform infrared spectroscopy; MBH, membrane-bound hydrogenase; TXRF, Total X-ray reflection fluorescence spectroscopy; XANES, X-ray absorption near-edge structure; XAS, X-ray absorption spectroscopy.

Acknowledgements

We thank the staff at the EMBL Outstation Hamburg and in particular Dr. W. Meyer-Klaucke for excellent support, Prof. R. Bittl and S. Keßler (FU-Berlin) for generous help with the EPR experiments of the MBH, and Dr. F. Lendzian and M. Saggiu for support in EPR experiments on *D. gigas*. Financial support from the Deutsche Forschungsgemeinschaft within SFB 498 (projects C1 and C8) is gratefully acknowledged.

Abstract

For the first time, the metal cofactors of the oxygen-tolerant membrane-bound Ni-Fe hydrogenase (MBH) of *Ralstonia eutropha* H16, were investigated by X-ray absorption spectroscopy (XAS). Measurements at the nickel K-edge were employed to study the atomic structure and the oxidation state of the Ni site in the MBH in its inactive as-isolated and hydrogen-activated forms. The Fe-S clusters were investigated by measurements at the iron K-edge. The MBH was compared to *Desulfovibrio gigas* standard hydrogenase which previously has been crystallized. Complementary to XAS, EPR spectroscopy was applied to characterize those states of the MBH and the *D. gigas* enzyme which contain Ni^{III}. Both, the Ni-Fe site and the Fe-S clusters of the oxygen-insensitive MBH revealed pronounced structural differences in comparison to the cofactors of *D. gigas* hydrogenase. The implications of these findings for the oxygen-tolerant catalytic behavior of the MBH are discussed.

Introduction

Hydrogenases are enzymes which catalyze the reversible cleavage of molecular hydrogen. The β -proteobacterium bacterium *Ralstonia eutropha* H16 houses three different Ni-Fe hydrogenases. These enzymes deviate from those found in anaerobic organisms because they are all functional under oxygen whereas the so-called standard Ni-Fe hydrogenases are completely inhibited by O₂ (Pierik *et al.* 1998). In previous investigations we have studied the RH and the SH enzymes of *R. eutropha* by X-ray absorption spectroscopy (XAS). The topic of the present work is the membrane-bound hydrogenase (MBH). Its physiological function is to feed electrons from H₂ cleavage into the respiratory chain by donating electrons to a membrane-integral cytochrome (Schink 1979; Bernhard *et al.* 1997; Happe *et al.* 1997). Accordingly this enzyme is predominantly active in hydrogen cleavage.

The MBH is composed of a large 67.1 kDa subunit that harbours the Ni-Fe complex which is the active site of hydrogen chemistry and a small 34.6 kDa subunit (Schneider *et al.* 1983; Podzuweit *et al.* 1987). On the basis of the amino acid sequence of the small subunit, it has been proposed that it binds three Fe-S clusters similar to standard Ni-Fe hydrogenases of, e. g. *D. gigas* (Schink 1979; Kortlüke *et al.* 1992; Bernhard *et al.* 1996). FTIR spectra of the MBH from *R. eutropha* have revealed a ligand complement at the Fe of the Ni-Fe site which is similar to the *D. gigas* enzyme, namely one CO and two CN⁻ molecules (Vincent *et al.* 2005a).

The catalytic features of the MBH previously have been studied. The specific activity of the isolated MBH strongly depends on the pH. The activity is maximal around pH 5.5 and decreases at alkaline pH, being about zero at pH 8. At variance with standard hydrogenases, the MBH is able to maintain significant hydrogen oxidation

activity (~70%) in the presence of atmospheric oxygen partial pressure (Vincent *et al.* 2005a; Vincent *et al.* 2005b). The activity recovers rapidly to the maximal level if O₂ is removed. The reasons for the remarkable oxygen-tolerance of the MBH, so far, are unclear.

The MBH is the only hydrogenase in *R. eutropha* that exhibits in its as-isolated form an EPR-signal due to a state containing Ni^{III}. In analogy to standard hydrogenases, this signal has been attributed to the so-called Ni-B state (Schneider *et al.* 1983; Knüttel *et al.* 1994) where presumably a hydroxide is bound in a bridging position between Ni and Fe. However, the Ni-A state which carries a bridging peroxide (Volbeda *et al.* 2005) has not been observed. During conversion to the active state by exposure to hydrogen, another Ni^{III} signal has been observed (Knüttel *et al.* 1994). This signal has been attributed to the Ni-C state where the bridging species is a hydride (Brecht *et al.* 2003). The Ni-C state is also found in the reduced regulatory hydrogenase (RH) of *R. eutropha* and in standard hydrogenases.

X-ray absorption spectroscopy is a sensitive tool to elucidate the atomic structure of metal sites in enzymes. In the present study, for the first time, various oxidation states of the membrane-bound hydrogenase of *R. eutropha* at different pH values were investigated by X-ray absorption spectroscopy (XAS). These measurements were complemented by EPR spectroscopy. By XAS measurements at the Ni K-edge information on the coordination and the oxidation state of the nickel atom in the active site was obtained. XAS at the Fe K-edge was used to investigate the Fe-S clusters. As a reference, the previously crystallized (Volbeda *et al.* 1995; Volbeda *et al.* 2005) standard Ni-Fe hydrogenase of *D. gigas* was studied.

Materials and Methods

Enzyme Purification and Characterization

Membrane-bound hydrogenase (MBH) protein from *Ralstonia eutropha* H16 was purified in the laboratory of B. Friedrich (Humboldt Universität, Berlin) as will be described in a forthcoming publication (Ludwig *et al.*, in prep.). The extracted protein was divided in two equal parts, 2x10 mL buffer S (50 mM KPO₄ buffer containing 10% glycerol) was added (samples at pH 5.5 and pH 7.0 were prepared). Finally, the protein was concentrated by ultrafiltration (Amicon Microcon (YM-10) centrifugal filter device (10,000 rpm, 2 x 20 min, 4°C) to a concentration of 53.7 mg/mL (pH5.5) and 62.2 mg/mL (pH7). The samples with a pH of 8 were purified as described in (Vincent *et al.* 2005a). After preparation, MBH samples were frozen and stored in liquid N₂.

Hydrogenase samples from *Desulfovibrio gigas* (~1.5 mM protein concentration) in phosphate buffer (pH 7.5) were obtained as outlined in (Cammack *et al.* 1994; DeLacey *et al.* 2004) and provided by Dr. A. DeLacey (Universidad Autonoma, Madrid).

Protein concentrations were determined according to (Bradford 1976). The H₂-oxidizing activity was quantified by an amperometric H₂-uptake assay using a H₂-electrode with methylene blue as an electron acceptor (Pierik *et al.* 1998).

Quantification of the nickel and iron contents of the MBH was performed by total reflection X-ray fluorescence spectroscopy (TXRF) on a Picotax spectrometer (Bruker) in our laboratory. The average metal contents of several samples were 1 ± 0.2 Ni and 9.7 ± 0.2 Fe per MBH protein.

Reductive Treatments and Sample Preparation

Prior to reduction, the concentrated protein solutions were thawed and degassed several times under nitrogen. MBH samples were reduced by incubation with 100 % hydrogen for 30 min at RT or by addition of Na-dithionite solution to a final concentration of 10 mM and incubation for 10 min at 20°C (RT). Samples of *D. gigas* were reduced by flushing with hydrogen gas for 3 hours at ~35°C. Approximately 20 µL of the samples were filled under Argon atmosphere into Kapton-covered sample holder (EPR and XAS measurements). The samples were frozen and stored in liquid nitrogen until use.

X-ray Absorption Spectroscopy

Fluorescence detected XAS spectra at the nickel and the iron K-edges (20K) were recorded at beamline D2 of the EMBL (HASYLAB, DESY, Hamburg, Germany) using a 13-element solid-state germanium detector (Canberra) during three measuring periods. Measurements were carried out as described in (Haumann *et al.* 2003; Buhrke *et al.* 2005; Burgdorf *et al.* 2005).

Fe XAS spectra were collected up to $k = 16.2 \text{ \AA}^{-1}$ (~1020 eV above $E_0=7112 \text{ eV}$). Ni XAS spectra were measured up to $k = 15 \text{ \AA}^{-1}$ (~850 eV above $E_0= 8333 \text{ eV}$) in MBH and up to $k = 15.4 \text{ \AA}^{-1}$ (~920 eV above $E_0= 8333 \text{ eV}$) in *D. gigas*. The Ni EXAFS spectra show a small Cu K-edge at ~9 KeV because of trace amounts of Cu in the samples. To remove the Cu contribution from the spectra, the Cu XAS spectrum was recorded in parallel to the Ni spectrum. Therefore the window of one of the 13 single channel analyzers was centered around the Cu K_α-fluorescence (12 channels were set to the Ni K_α-fluorescence). After energy calibration 15-20 scans for each Ni spectrum and 6-7 scans for each Fe spectrum were averaged for MBH and *D. gigas* samples. From Ni fluorescence spectra the respective weighted Cu fluorescence spectra were subtracted to eliminate the Cu contributions and to obtain a pure Ni spectrum (Gu *et al.* 2003).

The spectra were normalized, and EXAFS oscillations were extracted as described in (Dau *et al.* 2003). The energy scale was converted to a wavevector-scale (k -scale) using an E_0 value of 8333 eV for Ni and 7112 eV for Fe (Gu *et al.* 1996; Löscher *et al.* 2006). Unfiltered k^3 -weighted spectra were used for least squares curve fitting with the in-house software SimX (Dittmer 1999) and for calculation of Fourier

transforms (FTs) as previously (Haumann *et al.* 2003). For EXAFS simulations phase functions were calculated using FEFF 7 (Zabinsky *et al.* 1995). Pre-edge peak areas were extracted from normalized XANES spectra by subtraction of a polynomial spline from the main edge rise.

EPR Spectroscopy

EPR measurements on MBH samples in the X-band (microwave frequency of about 9.4 GHz) were carried out on a Bruker Eleksys E580 spectrometer equipped with a helium cryostat in the laboratory of Prof. R. Bittl (Freie Universität Berlin, Germany). EPR spectra of *D. gigas* hydrogenase were collected on a Bruker ESP 300E spectrometer equipped with a helium cryostat at 9.59 GHz microwave frequency (laboratory of Dr. F. Lenzian, Technische Universität Berlin, Germany). For further experimental details, see figure captions.

RESULTS

Characterization of the Ni-Fe site

Ni XANES

In the XANES region of XAS spectra, information on the ligands in the first coordination sphere of Ni is obtained. Figure 1 shows Ni XANES spectra of the MBH from *R. eutropha* at pH 5.5 (upper traces) and of the *D. gigas* hydrogenase (lower traces). Solid lines represent spectra of the as-isolated enzymes and open circles spectra of the hydrogen reduced enzymes, respectively.

The XANES spectra of the MBH and the *D. gigas* hydrogenase reveal an overall similar shape. However, the XANES spectrum of the oxidized MBH shows a higher primary edge maximum (at ~ 8341 eV) and a steeper edge slope in contrast to the oxidized *D. gigas* protein. The spectrum of the oxidized *D. gigas* enzyme (Fig. 1, lower traces, bold line) is similar to a previously published one (Gu *et al.* 1996). In combination with crystallographic data of this enzyme (Volbeda *et al.* 1995; Volbeda *et al.* 2005), this spectrum has been attributed to a five-coordinated Ni with four thiolate ligands from cysteines and one oxygen ligand in a bridging position between Ni and Fe (Gu *et al.* 1996; Gu *et al.* 2003). Reductive activation of the enzyme by hydrogen causes a slight decrease of the primary maximum of the XANES spectrum, reflecting the loss of the oxygen species and its replacement by a hydride at least in part of the preparation. That the edge maximum of the spectrum of oxidized MBH is larger than that of the *D. gigas* enzyme in the oxidized state suggests that more than one oxygen ligand is bound to the Ni. Under reducing conditions, a decrease of the primary edge maximum is observed and additionally a shoulder in the edge rise appears at ~ 8336 eV. We interpret these features as suggesting the loss of one oxygen ligand from the Ni in

part of the protein and binding of an H-species, in accord with previous results (Burgdorf *et al.* 2005) and with the *D. gigas* data.

The upper inset in Fig. 1 shows an enlargement of the shoulder in the MBH spectrum after hydrogen reduction. This feature is attributed to $1s \rightarrow 4p_z$ transitions found in square-pyramidal but not in trigonal-bipyramidal, five-coordinated Ni complexes (Colpas *et al.* 1991; Davidson *et al.* 2000).

The lower inset of Fig. 1 shows the pre-edge peak features at ~ 8332 eV which were extracted from the XANES spectra of oxidized MBH and *D. gigas* hydrogenase. The pre-edge peak is due to dipole-forbidden $1s \rightarrow 3d$ transitions and indicative of the local geometry at the Ni. The pre-edge peak area of the MBH is smaller and reveals only a single maximum compared to *D. gigas*, where two maxima are observed. These differences point to a more symmetric ligand arrangement around the Ni in the MBH.

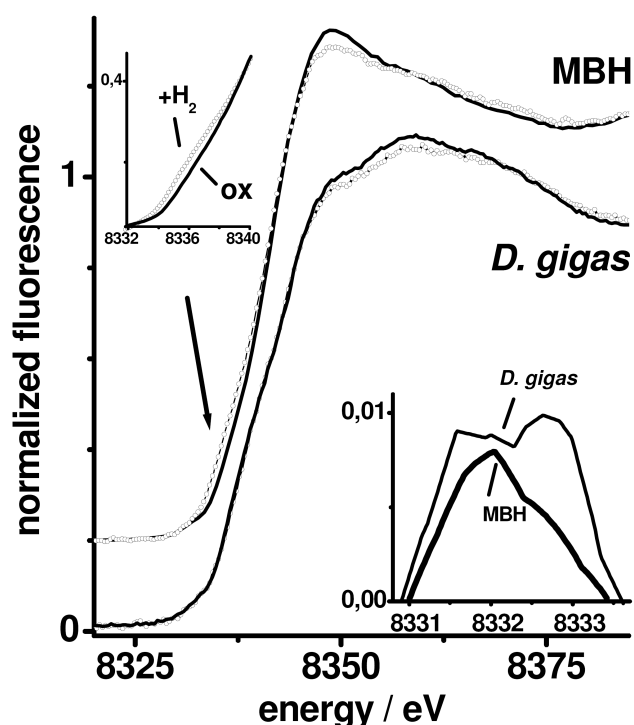


Figure 1: XANES spectra at the Ni K-edge of MBH and *D. gigas* hydrogenases in the oxidized and H₂-reduced state. Solid lines: oxidized; open circle lines: H₂-reduced. The upper inset shows the enlarged spectral region attributed to $1s \rightarrow 4p_z$ transitions at around 8336 eV marked by the arrow in the main trace. The lower inset shows the pre-edge peaks of the oxidized enzymes due to dipole-forbidden $1s \rightarrow 3d$ transitions. Bold line: MBH; thin line: *D. gigas*. The pre-edge peaks were extracted from the edge spectra as described in the Materials and Methods section.

Ni EXAFS

To gain more precise structural information on the Ni-site of the MBH, EXAFS spectra were analyzed. The EXAFS region bears information on the number and chemical identity of ligands, and on the Ni-ligand distances up to about 4 Å. Figure 2A shows the Fourier-transforms (FTs) of EXAFS spectra of MBH (upper spectra) and *D. gigas* hydrogenase (lower spectra) in the as-isolated and the H₂-reduced forms. Visual inspection of the spectra reveals that the FT amplitudes and the amplitudes of the corresponding EXAFS oscillations of the MBH are strongly reduced in comparison to the *D. gigas* enzyme.

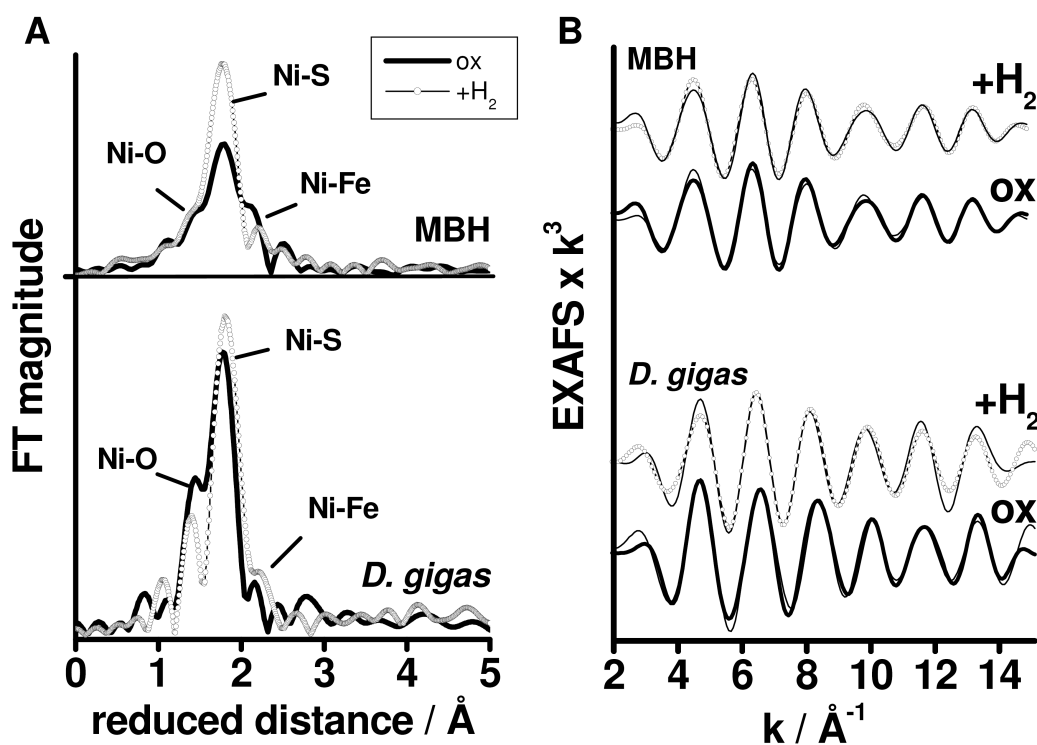


Figure 2: (A) Fourier-transforms of Ni EXAFS oscillations ranging up to $k = 15.4$ of the MBH of *R. eutropha* (upper spectra) and *D. gigas* hydrogenases (lower spectra) in the oxidized and H₂-reduced state (solid lines, oxidized; open circles, reduced). (B) Fourier-filtered EXAFS oscillations (a backtransform window of 0-3 Å of reduced distance was employed in the backtransformation of the FTs shown in (A)). Solid line and open circles: experimental spectra of MBH and *D. gigas* hydrogenase as in (A); thin lines: simulation curves. Spectra are vertically displaced for better comparison.

The FTs are dominated by a peak at ~ 1.8 Å of reduced distance (Fig. 4, the true metal-ligand distance is by ~ 0.4 Å larger). The resulting Ni ligand distance of ~ 2.3 Å is characteristic for Ni-S bonds (Gu *et al.* 2003). Under reducing conditions an increase of the dominant FT peak is observable, particularly in the MBH. In the oxidized forms of both preparations (dotted lines) a shoulder in the FT at ~ 1.5 Å is

observable. This shoulder presumably is due to contributions of Ni-O vectors. It is decreased in the reduced *D. gigas* enzyme (thick line), inline with the assumption that an oxygen species is removed from the Ni. A further feature of the FTs is the shoulder at reduced distances of about 2.2 Å (~2.6 Å true distance) in all spectra. It may be attributed to a Ni-Fe vector.

In this work, the *D. gigas* Ni spectra were used as a reference of the Ni-site because of the known structure from crystallographic data. Simulation of the *D. gigas* spectra yielded benchmarks, e. g. for Debye-Waller parameters. A reasonable fit of the *D. gigas* spectra was obtained using five backscatterer shells, namely O, 3xS, and Fe. The sulfur shell at a comparably large distance from the Fe was required for reasonable simulations including the Ni-Fe vector and resulted in an almost similar Ni-S distance of ~2.7 Å and a Ni-Fe distance of 2.8 Å in the oxidized *D. gigas* enzyme. The spectra of the as-isolated and reduced enzymes were simulated in a joint fit approach. The best-fit results are shown in Table 1.

The simulation results corroborate that an oxygen ligand is lost from the Ni upon H₂-reduction in the *D. gigas* enzyme. In H₂-reduced *D. gigas* enzyme, both the long Ni-S and the Ni-Fe vectors were shortened by ~0.2 Å. The obtained Ni-ligand distances are comparable to the crystallographically determined ones.

Table 1: Parameters for joint simulations of EXAFS oscillations at the Ni K-edge of MBH and *D. gigas* hydrogenase.

	shell	N_i [per Ni]	R_i [Å]	$2\sigma_i^2$ [Å ²]	R_F [%]
MBH ox/ +H ₂	O	2.27/0.99	2.19/1.98	0.003	20.9
	S	2*/2*	2.21/2.22	0.004*	
	S	1*/1*	2.38/2.39	0.004*	
	S	1*/1*	2.76/2.58	0.004*	
	Fe	1*/1*	2.79/2.60	0.009	
<i>D. gigas</i> ox/ +H ₂	O	1.1/0.2	1.86/2.00	0.003	18.2
	S	2*/2*	2.15/2.18	0.004 [#]	
	S	1*/1*	2.20/2.29	0.004 [#]	
	S	1*/1*	2.76/2.60	0.004 [#]	
	Fe	1*/1*	2.79/2.61	0.009	

The joint fits in *D. gigas* were performed with fixed integer values of the coordination numbers of S and Fe atoms (N_i), and a variable Ni-O vector. The Debye-Waller parameters ($2\sigma_i^2$) were also varied. The Debye-Waller factors derived for simulation of *D. gigas* spectra were used for subsequent simulations of the MBH. R_i , Ni-backscatterer distances; [#], Debye-Waller factors for Ni-S vectors in *D. gigas* simulation were set as equal; *, Parameters that were kept constant in the simulations.

We used a similar fit approach as in the *D. gigas* case to simulate the spectra of oxidized and H₂-reduced MBH. In contrast to the *D. gigas* case a fit with a Ni-O coordination number of close to one did not yield a reasonable fit (R_F of ~60%) (data not shown). An increase of the Ni-O coordination number by about one unit, as implied by the XANES data, was sufficient to obtain a reasonable fit result (R_F of ~21%). By varying the sulfur coordination numbers in the MBH no improvement of the fit was obtained (data not shown). The simulations reveal similar Ni-Fe distances in both, the MBH and the *D. gigas* enzyme. In addition, after reduction, a similar shortening of the Ni-Fe distance in MBH as in *D. gigas* is observed. Figure 2B displays the backtransforms into the k -space of Fourier isolates of MBH and *D. gigas* hydrogenase. The respective simulation curves corresponding to the parameters in Table 1 reveal the comparable fit quality in both cases.

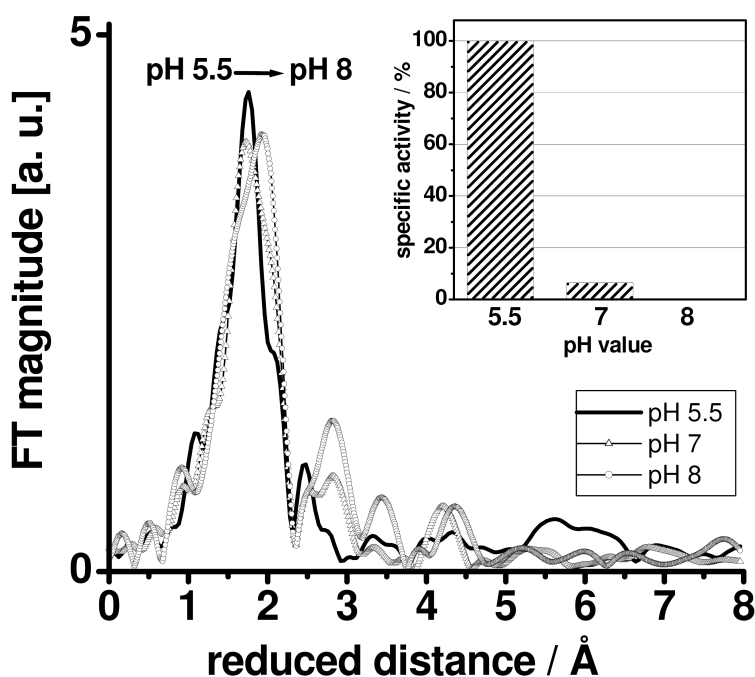


Figure 3: Fourier-transforms of EXAFS oscillations of the MBH at three pH values. Note the shift to larger distances of the main FT peak due to Ni-S vectors with increasing pH. The inset demonstrates that the specific activity is maximal at pH 5.5 and drops to zero at pH 8.

Figure 3 shows the FTs of EXAFS oscillations of the MBH at three pH values (5.5, 7, 8). A clear shift of the main FT peak to larger distances with increasing pH is observed. The inset of Fig. 3 demonstrates that the specific activity decreases at more alkaline pH. Simulations using the same fit approach as described above reveal comparable lengths of the Ni-Fe (2.8 Å) and Ni-O (2.09 Å) vectors at the three pH

values. The average Ni-S distance increases from 2.35 Å at pH 5.5 by about 0.2 Å to 2.55 Å at pH 8 (data not shown). Under reducing conditions a slight decrease in the average Ni-S distance is observable. The shortening of the Ni-Fe distance is obtained at pH 5.5 and 7, but not at pH 8, where the MBH is inactive (data not shown).

Spectroscopy on the Fe-S clusters

Fe XAS

To characterize the Fe-S clusters, Fe XAS spectra were measured. Figure 4 shows Fe XANES spectra (A) and the FTs of EXAFS spectra (B) of MBH and *D. gigas* enzymes. Both hydrogenases were measured in their as-isolated form. Again the *D. gigas* enzyme served as a reference because its Fe-S cluster complement is known. It consists of one [3Fe-4S] cluster and two [4Fe-4S] clusters (Volbeda *et al.* 1995). The XANES spectra of MBH and *D. gigas* were similar, suggesting predominant coordination of the Fe atoms by sulfur in both cases.

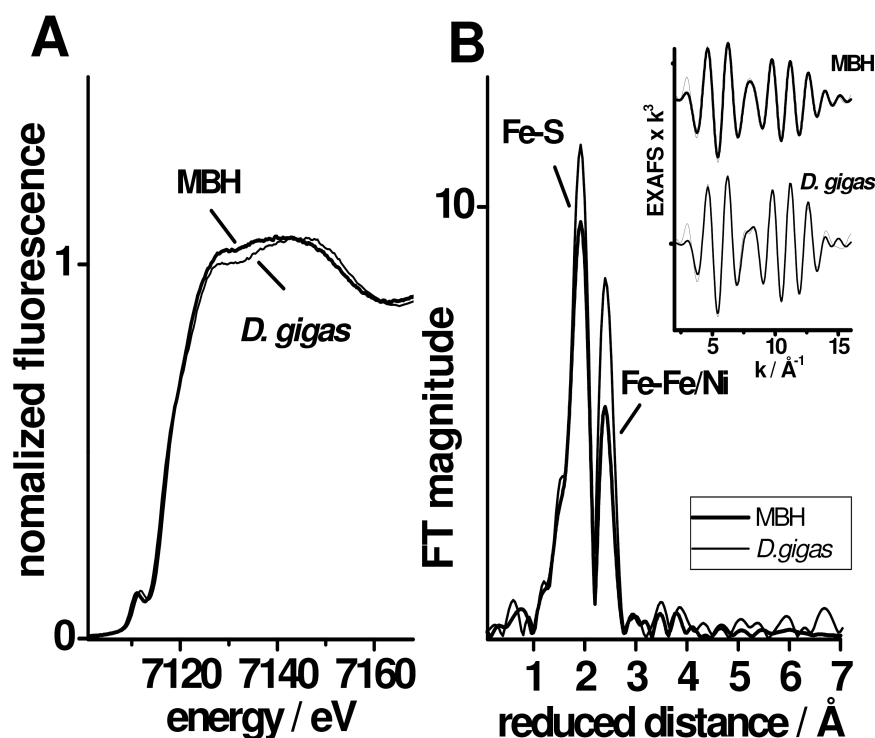


Figure 4: (A) Fe XANES spectra of as-isolated MBH (thick line) and *D. gigas* (thin line). (B) FTs of Fe EXAFS oscillations; the respective backtransforms (0-3 Å of reduced distance) with their simulations (gray lines) are shown in the inset (see Table 2).

However, visual inspection of the EXAFS Fourier-transforms (Fig. 4B) immediately reveals pronounced differences between the MBH and *D. gigas*. The FTs of Fe-S cluster EXAFS spectra show two prominent peaks in both enzymes. They are attributable to Fe-S (~2.2 Å) and Fe-Fe (~2.7 Å) interactions. In the MBH, the amplitudes of both FT peaks were reduced, meaning that there are fewer Fe-S and Fe-Fe interactions per Fe atom. These findings point to a different iron-sulfur cluster complement in the MBH compared to *D. gigas*.

Simulations of the EXAFS oscillations were carried out. The respective parameters are summarized in Table 2. In the simulations, two backscatterer shells were employed (Fe-S and Fe-Fe/Ni vectors, the Fe-Ni distance can not be discriminated from Fe-Fe interactions) (Table 2). In *D. gigas* the coordination number for the Fe-Fe/Ni vector was expected to be around 2.6 as calculated on the basis of the three Fe-S clusters (see above) and the Ni-Fe vector. Each iron of the two [4Fe-4S] clusters has three other irons as neighbors, in the [3Fe-4S] cluster the Fe has two irons as neighbors, and in the Fe-Ni site one metal neighbor has to be counted. The sum of the Fe-Fe/Ni bonds divided by the sum of the Fe atoms present in the *D. gigas* enzyme gives a calculated value of 2.58 for the Ni-Fe/Ni coordination number. Similarly, the value of the Ni-S coordination number of 3.75 was calculated. The iron atoms of the Fe-S cluster are coordinated each by four sulfurs, except one Fe of the [4Fe-4S] cluster which is bound by a histidine instead of a thiolate from a cysteine (known from crystallographic data); the Fe of the Ni-Fe site is coordinated by two S.

Table 2: Simulation parameters of EXAFS oscillations at the Fe K-edge of MBH and *D. gigas*.

	shell	N_i [per Fe]	R_i [Å]	$2\sigma_i^2$ [Å ²]	R_F [%]
MBH I/II	Fe	2.58*/1.5	2.72/2.71	0.009*/0.009*	39.5/10.6
	S	3.75*/3.2	2.28/2.28	0.008*/0.008*	
<i>D. gigas</i>	Fe	2.58*/2.4	2.71/2.71	0.009/0.009*	11.7/11.4
	S	3.75*/3.7	2.27/2.27	0.008/0.008*	

N_i , coordination numbers; R_i , Ni-backscatterer distances; $2\sigma_i^2$, Debye-Waller parameters. The following restraints were used in the simulations: *, Parameters that were kept constant in the simulations. MBH fits were performed, using the $2\sigma_i^2$ values obtained by simulations of the *D. gigas* enzyme.

The coordination numbers were fixed to their crystallographically determined values in the fit of the *D. gigas* spectrum. Such an approach yielded a reasonable fit quality ($R_F = 11.7\%$). The obtained Fe-Fe/Ni distances of 2.7 Å and Fe-S distances of 2.27 Å are typical for Fe-S clusters. Fixing the Debye-Waller parameters and varying

the coordination number (*D. gigas* Fit II) yielded similar iron-ligand distances but the coordination numbers are slightly reduced.

If the same parameters that accounted for the *D. gigas* spectrum were used to fit the MBH spectrum, unreasonable parameters were obtained. The error-sum (R_F) was more than three times larger ($R_F \sim 40\%$) (Table 2; MBH, Fit I). The fit was largely improved ($R_F = \sim 11\%$) if the coordination numbers were reduced (Debye-Waller parameters remained unchanged). Fit II of the MBH reveals coordination numbers of 1.5 for Ni-Fe/Ni and 3.2 for Ni-S. The Fe-Fe/Ni coordination number of 1.5, when taken at face value, is compatible with the presence of one [4Fe-4S], one [3Fe-4S], and one [2Fe-2S] cluster. The lower coordination number of the Fe-S interactions suggests that not all Fe atoms are coordinated by four sulfurs from terminal cysteines and bridging μ -S, but that there is nitrogen (or oxygen) ligation to a fraction of the Fe atoms. It is worth to note that the Fe XANES spectra, EXAFS oscillations, and respective Fourier-transforms obtained from MBH samples at different pH values were almost indistinguishable (data not shown). This means that an effect of the pH on the structure of the Fe-S clusters can be excluded.

EPR measurements to study the oxidation state of metal centers

The samples that were used for the XAS measurements previously were studied by EPR. Figure 5A shows the EPR spectrum at 60 K of the as-isolated MBH at pH 5.5 where activity is maximal. There are lines at g-values of 2.30, 2.17, 2.01 (see arrows) which are attributable to the Ni-B state (Schneider *et al.* 1983; Knüttel *et al.* 1994). Additional lines are discernible which previously have been proposed to result from magnetic interactions between the Ni^{III} of the Ni-B state and a further paramagnet, presumably a $[3Fe-4S]^+$ cluster (see below). A Ni-A signal was not detectable. Quantification of the number of Ni-B spins per MBH protein revealed that only about 10-20% were in the Ni-B state. The Ni-B signal was quantified by comparison with the Ni-A signal of *D. gigas*, assuming that Ni-A was present in 100% of *D. gigas* protein and taking the variations of the experimental parameters of the EPR measurements into account.

After reduction of the MBH by hydrogen flushing, the EPR spectrum changed drastically (Fig. 5B, upper trace). The Ni-B signal disappeared and a Ni-C signal became visible (g values of 2.20, 2.15, 2.01; see arrows). Further EPR signals from minor portions of Ni-B and the light-induced Ni-L state (g values of 2.25, 2.11, 2.05) were detectable. The Ni-L signal is observable by EPR, if the bridging hydride, found in the Ni-C state, is removed from the Ni by photo-dissociation (Van der Zwaan *et al.* 1985).

In contrast to the situation in the MBH, the *D. gigas* enzyme shows a Ni-A EPR signal in its oxidized state (Figure 5A, lower trace) which is converted to the Ni-C signal after exposure of the enzyme to hydrogen (Fig. 5B, lower trace). The respective g-values slightly differ from those in the MBH (Fig. 5, see legend). The differences in the EPR spectra in both enzymes point to structural and electronic differences of the Ni site of the MBH compared to *D. gigas* hydrogenase.

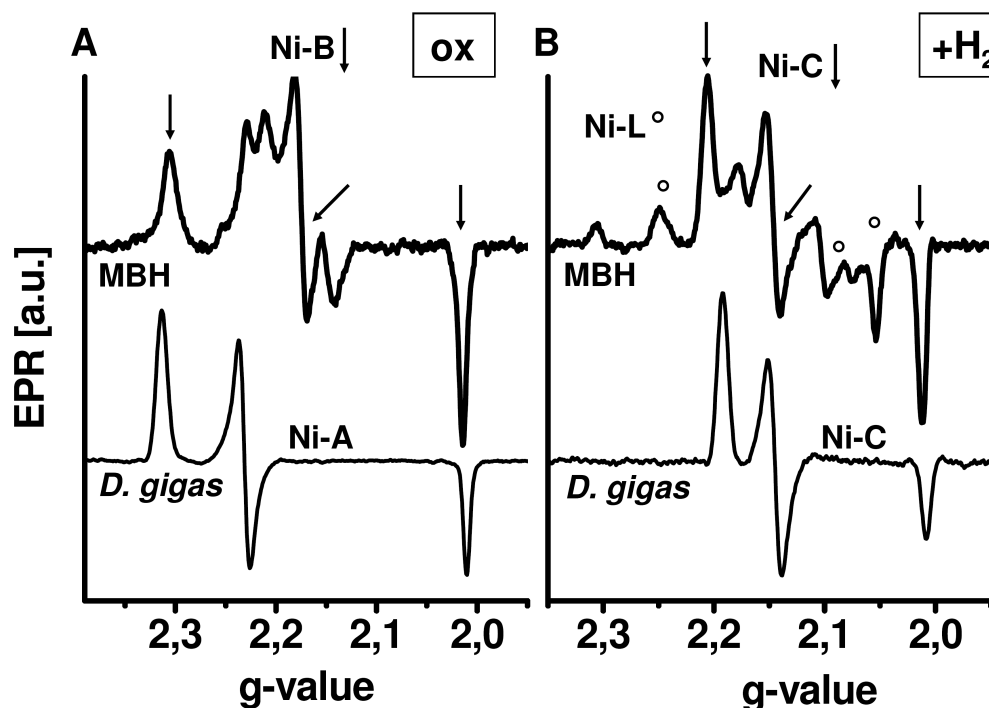


Figure 5: EPR spectra in the X-band of MBH (upper spectra) and *D. gigas* proteins (lower spectra) in the as-isolated (**A**) and H₂-reduced (**B**) states. (**A**) The oxidized MBH shows a Ni-B signal with g values of 2.30, 2.17, 2.01 (see arrows) and additional signals (g=2.23, 2.21, 2.14). The *D. gigas* sample shows a typical Ni-A signal. In the MBH (10-20%) Ni-B is present. (**B**) After hydrogen flushing, a Ni-C signal became detectable in the MBH (see arrows) in MBH. Small Ni-B and Ni-L (open circles) signals also are discernable. In the *D. gigas* enzyme, hydrogen flushing caused the conversion from the Ni-A state (g= 2.32, 2.23, 2.02) to the Ni-C state (g= 2.19, 2.16, 2.01). Spectra were approximately normalized according to the Ni-A signal of *D. gigas* hydrogenase for better comparison. EPR conditions: microwave power 1 mW; MBH at 60 K, *D. gigas* at 80 K.

Figure 6 shows EPR spectra of MBH enzyme (upper traces) and *D. gigas* hydrogenase (lower traces) at 10 K where contributions from Fe-S clusters are expected to be dominant. In Fig. 6A the spectra of the oxidized forms of both enzymes are compared. The *D. gigas* hydrogenase reveals a sharp signal at g=2.01 which has been attributed to the [3Fe-4S]¹⁺ cluster also found by crystallography. The MBH shows a

broadened asymmetric signal with the main line at $g=2.01$ as in *D. gigas*. In accord with the line splitting observed for the Ni-B signal, the line splitting found for the $[3\text{Fe-4S}]^{1+}$ cluster can be attributed to magnetic interactions between the Ni-Fe site in the Ni-B state and the $[3\text{Fe-4S}]^{1+}$ cluster.

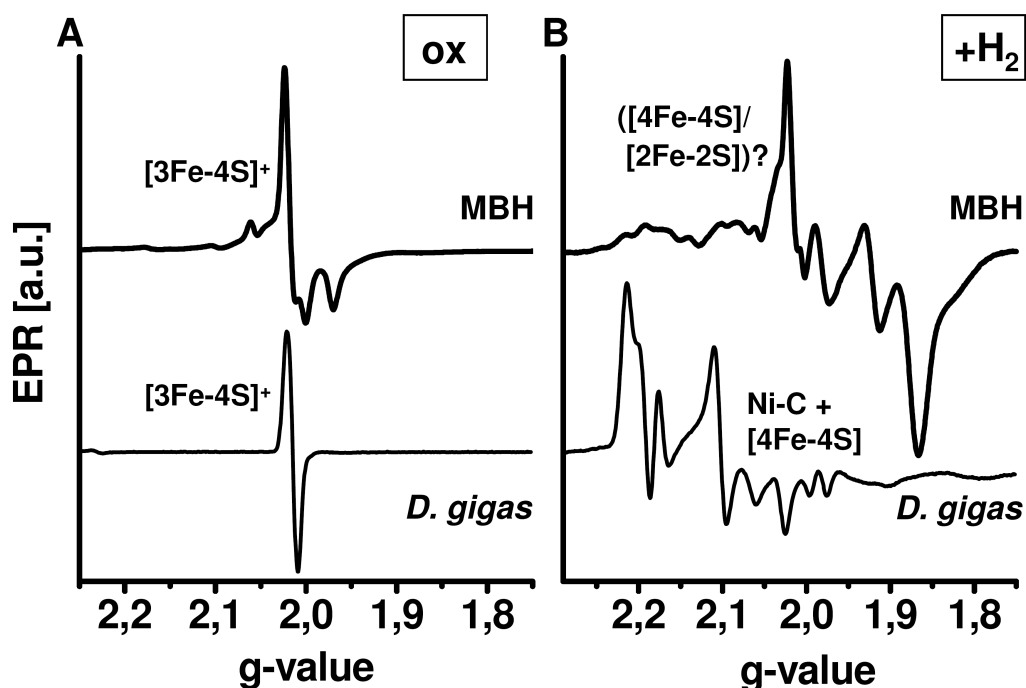


Figure 6: EPR spectra of the Fe-S cluster in the X-band of MBH (upper spectra) and *D. gigas* proteins (lower spectra) in the as-isolated (A) and H_2 -reduced (B) states. (A) Around $g=2.01$ the *D. gigas* shows a signal attributed to the $[3\text{Fe-4S}]^{1+}$ cluster. The signal in the oxidized MBH is attributed also to a $[3\text{Fe-4S}]^{1+}$ cluster which interacts with the Ni-B state in a fraction of enzymes. (B) Both enzymes show complex EPR spectra in their H_2 -reduced states. In *D. gigas* these signals have been attributed to a splitting of the Ni-C signal by spin-spin interaction with reduced Fe-S species (Teixeira *et al.* 1985; Cammack *et al.* 1987). The spectra were approximately normalized according to the sharp signal of *D. gigas* for better comparison. EPR conditions: microwave power 1 mW; MBH at 10 K, *D. gigas* oxidized at 10 K, H_2 -flushed at 6K.

EPR spectra of reduced MBH and *D. gigas* hydrogenase at low temperatures reveal features of the Fe-S clusters (Fig. 6B). In *D. gigas*, the complex low temperature spectrum (6K) has been proposed to result from magnetic interactions between the Ni-Fe site in the Ni-C state and reduced Fe-S species (Teixeira *et al.* 1985; Cammack *et al.* 1987). The EPR spectrum of the reduced MBH which is attributable to Fe-S clusters is completely different from that of the *D. gigas* enzyme. It may be due to reduced $[4\text{Fe-4S}]$ and/or $[2\text{Fe-2S}]$ species.

Discussion

The structure and oxidation state of the Ni-Fe site as revealed by XAS and the Fe-S cluster complement as characterized by XAS and EPR of the oxygen tolerant MBH of *R. eutropha* was compared to the situation in the standard hydrogenase of *D. gigas*. There are pronounced differences in the Ni-Fe site features and the Fe-S cluster composition between both enzymes. The spectroscopic results can be summarized as follows:

(1) By EPR spectroscopy it has been shown that in the as-isolated MBH no Ni-A state and only 10-20% of the Ni-B state is present. This is in contrast to the *D. gigas* hydrogenase, where in about 100% of the enzyme a Ni-A state has been observed. In the MBH possibly an EPR silent Ni-S state (without bridging oxygen species) may be predominant, depending on the redox potential. Hydrogen-reduction caused the conversion from a Ni-B to a Ni-C state in a fraction of the enzyme. However, the major fraction of the MBH was EPR silent. It may be present in a Ni-R like state, also depending on the redox potential. The Ni K-edge data are compatible with this interpretation. In a minor fraction of the MBH a loss of Ni-O species upon reduction has been detected. At ambient partial pressure of oxygen and corresponding redox potentials the Ni-A/B conformation seems to be destabilized in the MBH and the Ni-S form of the enzyme is favored. Hence, the active catalyst may be the prevailing form at ambient O₂ pressure.

(2) In the MBH 3-4 thiols from cysteines are likely bound to the Ni. The differences in the XAS data of MBH and *D. gigas* hydrogenase point to additional oxygen binding to the Ni in the MBH. In analogy to recent crystal structures and to the soluble hydrogenase of *R. eutropha* (SH), in the MBH sulfenates which are bound via their O-atom to the Ni may be present. That there is already O-ligation to Ni may destabilize bridging oxygen species and favour active catalyst conformation and hydrogen binding. This may be one reason for the O₂-tolerance of the MBH of *R. eutropha*.

(3) The XAS revealed that the pH value affects the conformation at the Ni in the active site of the MBH. At pH values where the MBH shows activity, the shortening of the Ni-Fe distance upon H₂-reduction may be a prerequisite for hydride binding.

(4) The XAS data of Fe-S clusters shows clear differences in the MBH compared to *D. gigas* enzyme which contains two [4Fe-4S] and one [3Fe-4S] clusters. The Fe-Fe coordination number in the MBH obtained by EXAFS simulations excludes such an Fe-S complement. XAS and EPR data of MBH is compatible with the presence of one [3Fe-4S] (seen by EPR), one [4Fe-4S], and one [2Fe-2S] cluster. Such an attribution is in line with the 9-10 iron atoms per MBH protein, determined by TXRF (see Materials and Methods). The [3Fe-4S] cluster may be in the proximal position in the MBH or at

least more close position to the Ni compared to *D. gigas* because it possibly magnetically interacts with the Ni^{III} in the Ni-B state. In contrast, in the *D. gigas* enzyme the [3Fe-4S] cluster is in the medial positioning and does not interact with Ni^{III} species. The functional role of the altered Fe-S cluster complement possibly is related to the binding of the MBH to cytochrome b in the membrane. However, at present it can not be excluded that a [2Fe-2S] cluster is formed as a degradation product of a [4Fe-4S] cluster during the protein purification procedure.

More detailed structural information on the MBH may become accessible if higher purity of intermediates is obtained. Redox titrations monitored by spectroscopic methods, namely XAS, EPR, and FTIR may shed light on the redox potential dependence of the intermediate states. In summary, we obtained the first XAS spectra of the Ni site and of the Fe-S clusters in the MBH. A basic characterization of the structural features of those metal sites has been achieved. The structural differences of the metal cofactors compared to the *D. gigas* hydrogenase may be related to the O₂-tolerant catalytic behavior of the MBH. Further investigations are required to clarify this issue.

References

- Bernhard, M., Benelli, B., Hochkoeppler, A., Zannoni, D. and Friedrich, B. (1997). "Functional and structural role of the cytochrome *b* subunit of the membrane-bound hydrogenase complex of *Alcaligenes eutrophus* H16" *Eur. J. Biochem.* **248**: 179-186.
- Bernhard, M., Schwartz, E., Rietdorf, J. and Friedrich, B. (1996). "The *Alcaligenes eutrophus* Membrane-Bound Hydrogenase Gene Locus Functions Involved in Maturation and Electron Transport Coupling" *J. Bacteriol.* **178** (15): 4522-4529.
- Bradford, M. (1976). "A Rapid and Sensitive Method for the Quantitation of Microgram Quantities of Protein Utilizing the Principle of Protein-Dye Binding" *Analytical Biochemistry* **72**: 248 - 254.
- Brecht, M., Van Gastel, M., Buhrke, T., Friedrich, B. and Lubitz, W. (2003). "Direct Detection of a Hydrogen Ligand in the [NiFe] Center of the Regulatory H₂-Sensing Hydrogenase from *Ralstonia eutropha* in Its Reduced State by HYSCORE and ENDOR Spectroscopy" *J. Am. Chem. Soc.* **125**: 13075 - 13083.
- Buhrke, T., Löscher, S., Lenz, O., Schlotter, E., Zebger, I., Andersen, L.-K., Hildebrandt, P., Dau, H., Friedrich, B. and Haumann, M. (2005). "Reduction of Unusual Iron-Sulfur Clusters in the H₂-sensing Regulatory Ni-Fe Hydrogenase from *Ralstonia eutropha* H16" *J. Bacteriol.* **280** (20): 19488-19495.
- Burgdorf, T., Löscher, S., Liebisch, P., Van der Linden, E., Galander, M., Lenzian, F., Meyer-Klaucke, W., Albracht, S. P. J., Friedrich, B., Dau, H. and Haumann, M. (2005). "Structural and oxidation-state changes at a non-standard Ni-Fe site during activation of the NAD-reducing hydrogenase from *Ralstonia eutropha* detected by X-ray absorption-, EPR-, and FTIR-spectroscopy." *J. Am. Chem. Soc.* **127**: 576-592.

- Cammack, R., Fernandez, V. M. and Hatchikian, E. C. (1994). "Nickel-Iron Hydrogenase" *Methods Enzymol* **243**: 43-68.
- Cammack, R., Patil, D., Hatchikian, E. C. and Fernandez, V. M. (1987). "Nickel and iron-sulfur centres in *Desulfovibrio gigas* hydrogenase: ESR spectra, redox properties and interactions" *Biochim. Biophys. Acta* **912**: 98-109.
- Colpas, G. J., Maroney, M. J., Bagyinka, C., Kumar, M., Willis, W. S., Suib, S. L., Mascharak, P. K. and Baidya, N. (1991). "X-ray spectroscopic studies of nickel complexes, with application to the structure of nickel sites in hydrogenases" *Inorg. Chem.* **30** (5): 920-928.
- Dau, H., Liebisch, P. and Haumann, M. (2003). "X-ray absorption spectroscopy to analyze nuclear geometry and electronic structure of biological metal centers—potential and questions examined with special focus on the tetra-nuclear manganese complex of oxygenic photosynthesis" *Analyt. Bioanalyt. Chem.* **376** (5): 562 - 583.
- Davidson, G., Choudhury, S. B., Gu, Z., Bose, K., Roseboom, W., Albracht, S. P. J. and Maroney, M. J. (2000). "Structural Examination of the Nickel Site in *Chromatium vinosum* Hydrogenase: Redox State Oscillations and Structural Changes Accompanying Reduktive Activation and CO Binding" *Biochemistry* **39**: 7468-7479.
- DeLacey, A. L., Pardo, A., Fernandez, V. M., Dementin, S., Adryanczyk-Perrier, G., Hatchikian, E. C. and Rousset, M. (2004). "FTIR spectroelectrochemical study of the activation and inactivation processes of [NiFe] hydrogenases: effects of solvent isotope replacement and site-directed mutagenesis" *J Biol Inorg Chem* **9**: 636-642.
- Dittmer, J. (1999). *Linear-Dichroismus-Röntgenabsorptionsspektroskopie zum katalytischen Zyklus des wasserspaltenden Mangan-Komplexes der Photosynthese in Theorie und Experiment*, Ph. D. Thesis, Christian Albrechts-Universität
- Gu, W., Jacquamet, L., Patil, D. S., Wang, H.-X., Evans, D. J., Smith, M. C., Millar, M., Koch, S., Eichhorn, D. M., Latimer, M. and Cramer, S. P. (2003). "Refinement of the nickel site structure in *Desulfovibrio gigas* hydrogenase using range-extended EXAFS spectroscopy" *Journal of Inorganic Biochemistry* **93**: 41-51.
- Gu, Z., Dong, J., Allan, C. B., Choudhury, S. B., Franco, R., Moura, J. J. G., Moura, I., Legall, J., Przybyla, A. E., Roseboom, W., Albracht, S. P. J., Axley, M. J., Scott, R. A. and Maroney, M. J. (1996). "Structure of the Ni Sites in Hydrogenases by X-ray Absorption Spectroscopy. Species Variation and the Effects of Redox Poise" *J. Am. Chem. Soc.* **118**: 11155-11165.
- Happe, R. P., Roseboom, W., Pierik, A. J., Albracht, S. P. J. and Bagley, K. A. (1997). "Biological activation of hydrogen" *Nature* **385** (6612): 126.
- Haumann, M., Porthun, A., Buhrke, T., Liebisch, P., Meyer-Klaucke, W., Friedrich, B. and Dau, H. (2003). "Hydrogen-Induced Structural Changes at the Nickel Site of the Regulatory [NiFe] Hydrogenase from *Ralstonia eutropha* Detected by X-ray Absorption Spectroscopy." *Biochemistry* **42** (37): 11004-15.
- Knüttel, H., Schneider, K., Erkens, A., Plass, W., Müller, A., Bill, E. and Trautwein, A. X. (1994). "Redox Properties of the Metal Centres in the Membrane-Bound Hydrogenase from *Alcaligenes eutrophus* CH34" *Bulletin of the Polish Academy of Science Chemistry* **42** (4): 495-511.

- Kortlüke, C., Horstmann, K., Schwartz, E., Rohde, M., Binsack, R. and Friedrich, B. (1992). "A Gene Complex Coding for the Membrane-Bound Hydrogenase of *Alcaligenes eutrophus* H16" *J. Bacteriol.* **174** (19): 6277-6289.
- Löschner, S., Burgdorf, T., Zebger, I., Hildebrandt, P., Dau, H., Friedrich, B. and Haumann, M. (2006). "Bias from H₂ Cleavage to Production and Coordination Changes at the Ni-Fe Active Site in the NAD⁺-Reducing Hydrogenase from *Ralstonia eutropha*" *Biochem.* **45**: 11658-11665.
- Ludwig, M. and Friedrich, B.: in preparation.
- Pierik, A. J., Schmelz, M., Lenz, O., Friedrich, B. and Albracht, S. P. J. (1998). "Characterization of the active site of a hydrogen sensor from *Alcaligenes eutrophus*" *FEBS Letters* **438**: 231-235.
- Podzuweit, H. G., Schneider, K. and Knüttel, H. (1987). "Comparison of the membrane-bound hydrogenases from *Alcaligenes eutrophus* H16 and *Alcaligenes eutrophus* type strain" *Biochim. Biophys. Acta* **905**: 435-446.
- Schink, B. S., H. G. (1979). "The membrane-bound hydrogenase of *Alcaligenes eutrophus*. I. Solubilization, purification, and biochemical properties" *Biochim. Biophys. Acta* **567** (2): 315-324.
- Schneider, K., Patil, D. and Cammack, R. (1983). "ESR Properties of Membrane-Bound Hydrogenases from aerobic Hydrogen Bacteria" *Biochim. Biophys. Acta* **748**: 353-361.
- Teixeira, M., Moura, I., Xavier, A. V., Huynh, B. H., DerVartanian, D. V., Peck, H. D. J., Legall, J. and Moura, J. J. G. (1985). "Electron Paramagnetic Resonance Studies on the Mechanism of Activation and the Catalytic Cycle of the Nickel-containing Hydrogenase from *Desulfovibrio gigas*" *J. Biol. Chem.* **260** (15): 8942-8950.
- Van der Zwaan, J. W., Albracht, S. P. J., Fontijn, R. D. and Slater, E. C. (1985). "Monovalent nickel in hydrogenase from *Chromatium vinosum*. Light sensitivity and evidence for direct interaction with hydrogen." *FEBS Letters* **179** (2): 271-277.
- Vincent, K. A., Cracknell, J. A., Lenz, O., Zebger, I., Friedrich, B. and Armstrong, F. A. (2005a). "Electrocatalytic hydrogen oxidation by an enzyme at high carbon monoxide or oxygen levels" *PNAS* **102** (47): 16951-16954.
- Vincent, K. A., Parkin, A., Lenz, O., Albracht, S. P. J., Fontecilla-Camps, J. C., cammack, R., Friedrich, B. and Armstrong, F. A. (2005b). "Electrochemical Definitions of O₂ Sensitivity and Oxidative Inactivation in Hydrogenases" *J Am Chem Soc.* **127**: 18179-18188.
- Volbeda, A., Charon, M. H., Piras, C., Hatchikian, E. C., Frey, M. and Fontecilla-Camps, J. C. (1995). "Crystal structure of the nickel-iron hydrogenase from *Desulfovibrio gigas*" *Nature* **373** (6515): 556-557.
- Volbeda, A., Martin, L., Cavazza, C., Matho, M., Faber, B. W., Roseboom, W., Albracht, S. P. J., Garcin, G., Rousset, M. and Fontecilla-Camps, J. C. (2005). "Structural differences between the ready and unready oxidized states of [NiFe] hydrogenases" *J. Biol. Inorg. Chem.* **10**: 239-249.
- Zabinsky, S. I., Rehr, J. J., Aukudinov, A., Albers, R. C. and Eller, M. J. (1995). "Multiple-scattering calculations of x-ray-absorption spectra" *Phys. Rev. B* **52** (4): 2995-3009.

